2024

Transport and Fate of Nitrate in a Saturated Buffer Zone as Assessed With a Chloride Tracer Test

Alhassan Sahad
Illinois State University

Eric W. Peterson
Illinois State University, ewpeter@ilstu.edu

Recommended Citation

Sahad, A., & Peterson, E.W. (2024). Transport and fate of nitrate in a saturated buffer zone as assessed with a chloride tracer test. Environmental & Engineering Geoscience 30(3): 161-171. https://doi.org/10.21663/EEG-D-23-00078

THE GEOLOGICAL SOCIETY OF AMERICA®

Open Access Article

Transport and Fate of Nitrate in a Saturated Buffer Zone as Assessed With a Chloride Tracer Test

ALHASSAN SAHAD[1] AND ERIC W. PETERSON*

Department of Geography, Geology, and the Environment, Illinois State University, Campus Box 4400, Normal, IL 61790

Key Terms: ***Nitrate, Saturated Buffer Zone, Tracer Test, Denitrification, Plant Uptake, End-Member Mixing, Tile Drainage***

ABSTRACT

The Upper Mississippi Basin, which includes Illinois, has highly fertile soils and experiences intensive agricultural practices. Although fertile, the soils do not drain well, resulting in the installation of tile-drainage systems. The practices of tile systems coupled with the application of nitrogen-rich fertilizers have led to the excessive export of nitrate from the agricultural fields into surface waters, contributing to eutrophication and the development of hypoxic zones in aquatic environments. Saturated riparian buffer zones (SRBs) have been proposed as a means to reduce the amount of nitrate discharged from tile-drained waters into streams. Previous works show a reduction in the nitrate as waters travel through an SRB, but *in situ* measurements of travel times are limited. Using the results from a 52-day tracer test, we developed a mathematical model combining end-member mixing of a tracer, chloride, and concentrations of nitrate as nitrogen (NO_3-N) to determine the travel time of the tile waters in an SRB and to quantify the amount of NO_3-N reduction occurring within an SRB. For the first 30 days, dissolved oxygen (DO) concentrations indicated aerobic conditions within the waters of most of the SRB, which saw a concomitant increase in NO_3-N concentrations along groundwater pathways. As DO concentrations decreased below 4.5 mg/L, NO_3-N concentrations began to lower along the flow pathways, resulting in NO_3-N reductions ranging from 23 to 97 percent.

INTRODUCTION

Agriculture is a leading contributor of surface water pollution, contributing nutrients such as nitrogen (N), to aquatic environments (Anderson et al., 2014). N is a primary nutrient required for the growth and development of plants. The need to increase crop yield has led to the increased application of N-based fertilizers to agricultural fields (Lemke et al., 2011; Miller et al., 2011; and Robertson and Saad, 2013). Concomitant with the increased application, nitrate as nitrogen (NO_3-N) concentrations in rivers and reservoirs throughout agricultural regions have risen (Gentry et al., 1998; David and Gentry, 2000). N-fertilizers and organic nitrogen in manure are major sources of nitrogen pollution as crops do not assimilate all of the applied N (Lutz et al., 2020).

The use of N-fertilizers in the Midwest of the United States has increased since the mid-20th century. Not all of the N-fertilizer is utilized by the crops, which has led to elevated concentrations of nitrate in surface waters (Peterson et al., 2001). Excessive nitrate accumulation degrades freshwater systems and causes changes to biodiversity and the death of aquatic organisms (David and Gentry, 2000). For example, the waters within the Mississippi River Basin register some of the highest concentrations of nonpoint source nitrate (NO_3^-) in the world (Hypoxia Task Force, 2018). The algal blooms and hypoxic zones in the Gulf of Mexico and Lake Erie illustrate clear manifestation of the negative impact of NO_3^- export into water bodies. According to Keeney and Hatfield (2008), the Illinois River, a tributary of the Mississippi River, contributes from 15 to 20 percent of the total nitrogen that is transported into the Gulf of Mexico.

In the Midwest region, particularly in Illinois, the soil typically has a high water table that hinders the growth of most crops. Excessive soil moisture stunts plant growth due to an oxygen deficiency in the root zone and a reduction in nitrogen uptake resulting from denitrification and leaching (Kaur et al., 2017). To improve soil drainage and increase crop yield, farmers have installed subsurface draining systems (tiles) to drain the soil water directly into surface water bodies (Fausey et al., 1995). However, the tiles short-circuit the roles of the soil in the nitrogen cycle, reducing or eliminating the opportunity for denitrification, plant uptake, and microbial immobilization. Whereas the installation of tile drains has successfully opened additional lands for agricultural developments and increased crop yield, the short-circuiting process directly contributes to 52 percent of nitrate entering the Gulf of Mexico (David and Gentry, 2000). Removal of the tile drains to protect water

[1]Present address: Institute for Data Science and Informatics, University of Missouri-Columbia, 22 Heinkel Building, Columbia, MO, 65211
*Corresponding author email: ewpeter@ilstu.edu

bodies is not practical; thus, a solution must be found to mitigate the negative impact of tiles on water quality.

In 2008, a national strategy action plan was implemented to address hypoxia in the Northern Gulf of Mexico and to improve water quality in the Mississippi River Basin (USEPA, 2017). In 2015, Illinois developed its own plan, the Illinois Nutrient Loss Reduction Strategy, with the goal of reducing nitrogen and phosphorus loads by 45 percent in the long term, and interim goals of 15 percent reduction in nitrate and 25 percent reduction in phosphorus by 2025 (IEPA et al., 2019). Four best management practices for agricultural nonpoint sources were proposed to achieve these goals: free water surface–constructed wetlands, denitrifying bioreactors, controlled drainage, and saturated riparian buffer zones (SRBs) (Carstensen et al., 2020). With an SRB, tile-drain water is redirected into a riparian buffer zone where the water travels as groundwater to the stream. While being transported through an SRB, the nitrogen-rich waters encounter conditions favorable for denitrification, assimilation, plant uptake, and dilution of the nitrate (Jaynes and Isenhart, 2014; Carstensen et al., 2020).

In the Midwest, widely implementing SRBs could result in a 5 to 10 percent reduction of the estimated N load from land drained by tile systems (Chandrasoma et al., 2019). However, the reported efficiencies of SRBs to reduce N loading has been highly variable. After monitoring six SRBs in Iowa with 17 site-years of data, Jaynes and Isenhart (2019) reported nitrate removal between 8 and 84 percent. Groh et al. (2019), monitoring three SRBs in the Midwest, concluded that cumulative denitrification could account for up to 77.3 percent of total nitrate removed. For a period from September 2016 to February 2017, Brooks and Jaynes (2017) observed 61 percent loss of nitrate loading across seven active buffers in Iowa, Illinois, and Minnesota. SRBs have been shown to lower NO_3-N concentrations through denitrification, plant uptake, and dilution (Jaynes and Isenhart, 2014; Groh et al., 2019; Miller et al., 2019; and Bosompemaa et al., 2021).

Research concerning the use of SRBs as means to remove nitrate from agricultural waters has highlighted the variability among systems to reduce nitrate. One aspect associated with removal is the travel time of the water within the SRB, which has been reported on the order of weeks (Jaynes and Isenhart, 2019). This work reports the use of a tracer test to identify travel times of diverted tile water through an SRB and the use of the tracer test data coupled with an end-member mixing model to assess the fate of the nitrate. The results highlight the heterogeneity of the system and suggest that the loss of nitrate is spatially and temporally variable.

MATERIALS AND METHODS

Study Site Description

The study area is in central Illinois (40.614382°N, 89.023542°W) and encompasses a floodplain that was once farmed but has been restored to a grassland (Figure 1). A third order stream, Tributary 3 (T3), serves as the western boundary of the study area. Similar to other Illinois streams (Mattingly et al., 1993; Becker and Peterson, 2022), T3 has been modified and receives tile drainage from a tile system draining a field to the east. The segment of stream adjacent to the site has not been modified in the last 30 years. The agricultural field is located approximately 90 m to the east and is separated from the property by a county road.

Across the site, the surface material (0–0.6 m) is dark organic-rich topsoil, which is underlain by a clay loam (0.6–1.5 m). Between 1.5 and 2 m, the clay loam coarsens with an increasing sand and gravel percentage. The coarse-grained medium is underlain by blue-gray, dense diamicton belonging to the Tiskilwa Till member of the Wedron Formation deposited during the Wisconsin glaciation (Weedman et al., 2014). The thickness of the diamicton in the region ranges from 30 to 45 m terminating at Silurian dolomite bedrock (Wickham et al., 1988). The organic matter content in the top 60 cm is 6.0 percent but decreases to 2 percent at a depth of 90 cm (Sanks et al., 2015; Bosompemaa et al., 2021).

Surface water infiltrates through the soils to the sand and gravel zone where it then flows horizontally. The sand and gravel waters represent the "shallow" waters, whereas the waters obtained from the diamicton are referred to as "diamicton" waters. The shallow and the diamicton waters have distinct geochemical signatures. Waters in the sand and gravel zone are a bicarbonate-rich water as compared with waters derived from the diamicton, which are sulfate-rich (Akara et al., 2016). The sand and gravel zone has a hydraulic conductivity (K) value of 2.2×10^{-5} m/s, calculated from the geometric mean of slug test results from 17 wells. At a depth of 1 m, the average porosity is 0.32 (Sanks et al., 2015). The depth to groundwater is approximately 2 m during the dry season and less than 0.5 m during the rainy seasons when the tile is running. Locally, the groundwater flows from the east to west with flow toward the stream T3 (Figure 1).

The study site has been modified with the installation of an agricultural treatment system (control box) that directs the tile water (agricultural runoff) into the subsurface within the riparian area, creating an SRB. The control box consists of three chambers separated by a set of stoplogs. The stoplog between the upper and middle chambers has a 45° v-notched weir that is positioned 0.18 m below the land surface; the elevation of the weir is 227.85 m above mean sea level (m.a.m.s.l.). The upper chamber receives the agricultural runoff, whereas the middle chamber redirects the water into a 15-cm outlet pipe that bifurcates into three distribution tiles positioned 1 m below the surface. The three tiles have individual lengths of 95 m (eastern tile), 110 m (middle tile), and 50 m (western tile) (Figure 1). The distance from the stream,

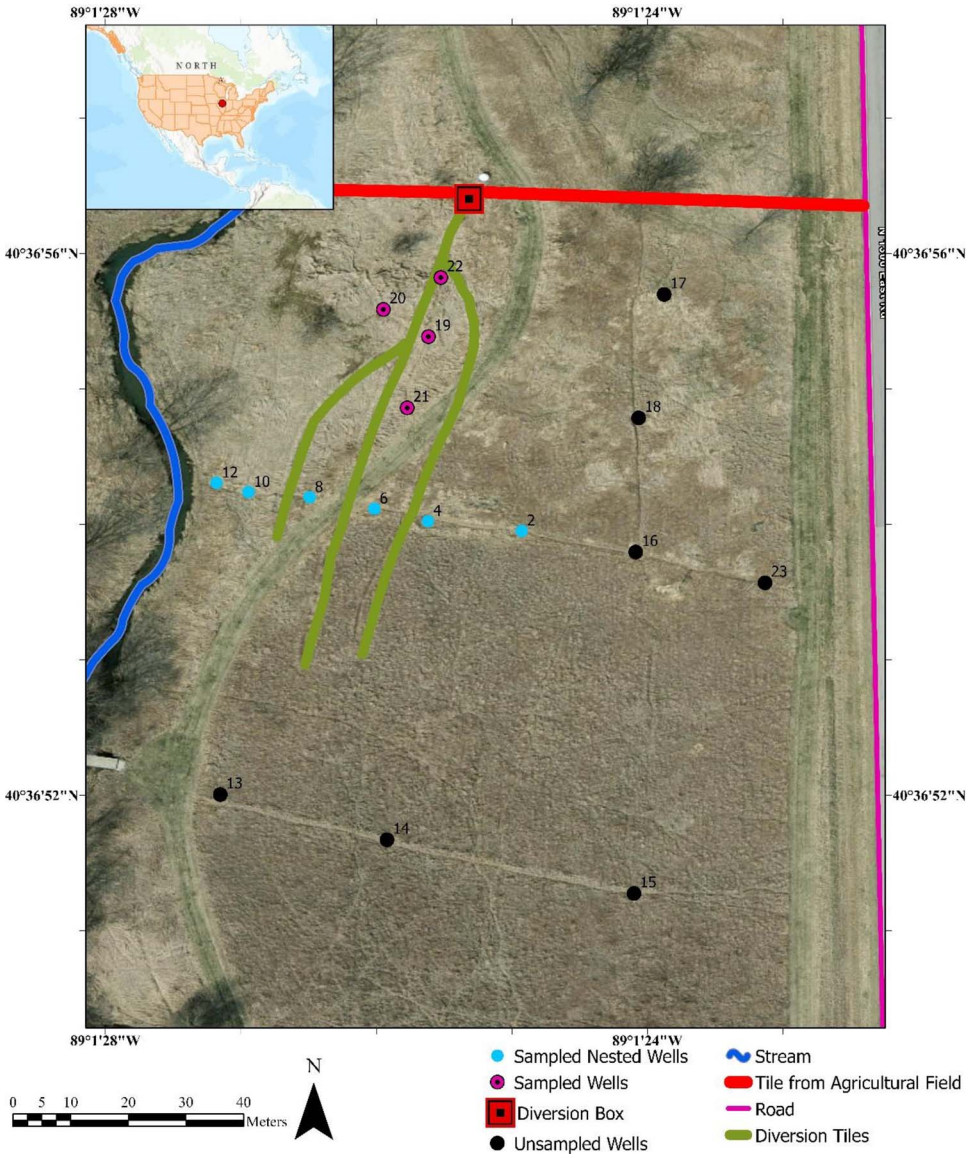

Figure 1. Illustration of the T3 SRB study site. The location of the monitoring wells, control (diversion) box, diversion tiles, and stream (T3) are noted. Sampled wells included 4C, 4D, 6C, 6D, 8C, 8D, 10C, 10D, 12C, 12D, 19, 20, 21, and 22.

which has a water surface elevation of approximately 225.70 m.a.m.s.l. when the tile is running, to the closest tile varies, ranging from roughly 15 m to slightly more than 50 m in distance. The system is designed to deliver excess tile water to the stream when the tile discharge exceeds the capacity of the middle chamber; however, continuous monitoring indicates that water has not breached the middle chamber. Thus, all water entering the middle chamber is delivered to the distribution tile system. The tiles start to run from late winter (late February–early March) to late spring (late May–early June).

Within the study site, 35 observation wells have been installed; each well has a 0.75-m long screen. A series of nested wells, wells 2, 4, 6, 8, 10, and 12, are aligned with groundwater flow and intersect the distribution tiles (Figure 1). The nested wells consist of four wells, labeled A through D. The A and B wells, installed to a depth of 3.8 and 3.0 m, respectively, allow collection of water from the diamicton. Wells C and D have screened depths that end at 2.3 and 1.5 m, respectively, and are designed to collect groundwater samples from the sand and gravel zone. The other 11 wells are screened to a 2.3-m depth. The vertical hydraulic gradient calculated from the nested wells 2, 4, 6, and 8 consistently have a downward vertical gradient, whereas, near wells 10 and 12, an upwelling of waters from the diamicton into the sand and gravel zone has been observed. Water chemistry data confirm the upwelling and indicate that upwelling may also occur near well 20 (Akara et al., 2016).

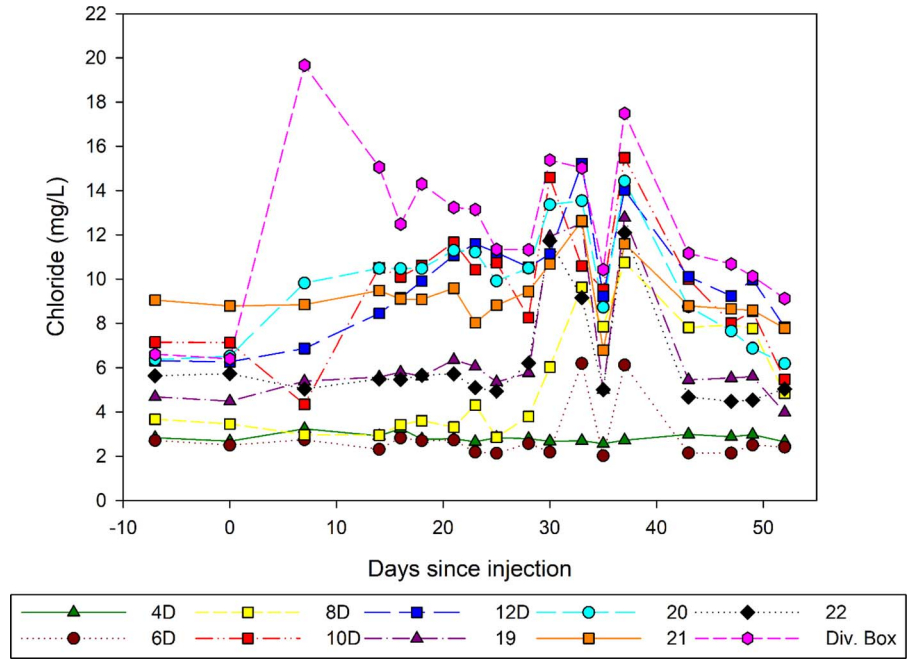

Figure 2. Time series graph of chloride concentrations measured in waters of the wells and the diversion box. The sampling on day -7 occurred 7 days prior to the injection. The sample at the diversion box on day 0 was pre-tracer injection.

Tracer Test

A tracer test was conducted within the SRB in the spring of 2021. The tracer test started on March 9, 2021 (day 0) following sustained flow within the tile for the previous seven days. Six kilograms of sodium chloride (NaCl) were mixed with 19 L of water and added to the upper chamber of the control box. The injection into the upper chamber of the control box allowed for the incoming tile water to further mix with the tracer solution before entering into the middle compartment, where it was diverted into the SRB through the diversion tiles.

Pre- and Post-Tracer Test Sampling

Groundwater samples were taken from the wells within the SRB and the control box prior to the start of the tracer test to ascertain the background concentration of the major anions. The first sampling post-injection occurred after 7 days on March 16, and sampling continued for 52 days following injection. Precipitation (recharge) events occurred on days 24 and 34. The recharge events impacted the breakthrough curves for the Cl^- (Figure 2). For all locations, *in situ* water quality parameters, including specific conductance, dissolved oxygen (DO), and temperature, were recorded using a YSI 85 probe. Water level measurements in the wells were recorded with an electronic water tape. Prior to sample collection, the wells were purged for stabilization of the *in situ* parameters. From each sampled well, withdrawn water was filtered through a 1-μm glass fiber filter and collected in 60-mL high-density polyethylene containers. Samples were stored on ice in the field and while in transit. Samples were stored at 4°C until being analyzed using a DIONEX ICS-1100 ion chromatograph for major anions, chloride (Cl^-), bromide (Br^-), nitrate as nitrogen (NO_3-N), and sulfate (SO_4^{2-}) following the U.S. Environmental Protection Agency method 300.1 (Hautman and Munch, 1997).

Post-tracer groundwater sampling started 7 days after the initiation of the tracer test. Initially, the planned sampling frequency was once a week; however, the first sampling revealed elevated Cl^- concentrations in a well, and the sample frequency increased to three times a week. Each sampling event followed the same protocol as the pretest sampling. Samples were collected from wells 4C, 4D, 6C, 6D, 8C, 8D, 10C, 10D, 12C, 12D, 19, 20, 21, and 22 during the 52-day study duration.

Chloride Travel Time

Breakthrough curve analysis was used to calculate the travel time of Cl^-. The mean velocity ($\underline{v}$) of flow of the tile water from a diversion tile to a well was calculated as:

$$\underline{v} = \frac{d}{t_P}, \tag{1}$$

where d is the distance from the upgradient tile to the well and t_p is the time to peak Cl^- concentration identified on the breakthrough curve. The hydraulic conductivity (K) was determined using Darcy's law:

$$K = \frac{(\underline{v} \times n)}{i}, \quad (2)$$

where n is the effective porosity of the aquifer and i is the hydraulic gradient. During the tracer test, the horizontal hydraulic gradient (i) across the study area was 0.002 m/m. The hydraulic conductivity values calculated using Darcy's law were compared to slug test–derived K values using a paired t-test ($\alpha = 0.05$) as a validation of the tracer test.

End-Member Mixing Model

Whereas Cl^- is a conservative anion, an anion with little to no loss from chemical reactions or sorption in the groundwater, the NO_3-N may not behave conservatively as it can be added or removed from the system. An end-member, two-component, mixing model was used to assess the transport and fate of nitrate (Triska et al., 1989). The end components were represented by the upgradient groundwater (g) and by the water in the control box (t), which mixed to produce the waters of the observed well (w). Two equations were employed:

$$Q_w = Q_t + Q_g, \quad (3)$$

$$Q_w \times Cl_w = (Q_t \times Cl_t) + (Q_g \times Cl_g), \quad (4)$$

where Q_w, Q_t, and Q_g represent the volume of water for each component and Cl_w, Cl_t, and Cl_g are the concentrations of Cl^- in the observed well, control box, and upgradient groundwater, respectively. The volume of water in the well and groundwater were not known, but combining Eqs. (3) and (4) allows for the proportion of tile water to water at the well to be calculated:

$$\frac{Qt}{Qw} = \frac{(Cl_w - Cl_g)}{(Cl_t - Cl_g)}. \quad (5)$$

Assuming a conservative nature for nitrate and substituting the concentration of NO_3-N for Cl^-, Eq. (5) can be rearranged to calculate the expected concentration of NO_3-N in an observed well (NO_3-N_w):

$$NO_3 - N_w = \left[\frac{Qt}{Qw} \times (NO_3 - N_t - NO_3 - N_g)\right] + NO_3 - N_g. \quad (6)$$

The concentrations calculated for the well (NO_3-N_w) represented the theoretical NO_3-N concentration assuming dilution is the only mechanism acting on the NO_3-N. However, nitrate is not conservative and can be added via nitrification and removed through denitrification or plant uptake from an SRB. Differences between the modeled NO_3-N_w concentrations, Eq. (6), and the measured NO_3-N concentrations quantify the loss or gain of nitrate from the water as it travels from the control box to the observed wells. A measured NO_3-N concentration for a given well that is greater than the modeled concentration from Eq. (6) implies that there is addition of nitrate, i.e., nitrification. A measured concentration less than the modeled concentration indicates nitrate removal, which could be due to denitrification or plant uptake.

Table 1. *Summary statistics for the chloride concentrations among the well waters of the SRB.*

	Chloride (mg/L)		
Well	Minimum	Mean ± Standard Deviation	Maximum
4C	2.90	3.60 ± 0.44	4.28
4D	2.57	2.83 ± 0.19	3.26
6C	2.12	3.14 ± 1.21	6.45
6D	2.02	2.85 ± 1.23	6.19
8C	2.66	5.90 ± 2.97	12.39
8D	2.86	5.49 ± 2.52	10.75
10C	4.62	6.97 ± 1.67	10.25
10D	4.35	9.82 ± 2.66	15.49
12C	5.69	9.98 ± 2.49	15.33
12D	6.26	10.10 ± 2.20	15.21
19	3.98	6.66 ± 2.71	12.77
20	6.19	10.01 ± 2.33	14.42
21	6.80	9.21 ± 1.34	12.63
22	4.48	6.24 ± 2.31	12.09

RESULTS

Chloride Data

The background concentration of the Cl^- in the groundwater and the waters of the control box were stable prior to the start of the test (Figure 2). After injection, concentrations in the waters of the downgradient wells increased, whereas the concentrations within the waters of the control box decreased. The concentrations of the Cl^- in the groundwater as measured from the wells downstream of the diversion tile ranged from as low as 2.02 mg/L to a maximum of 15.49 mg/L (Table 1). Wells 4C and 4D exhibited no elevated Cl^- concentrations, whereas wells 6C and 6D experienced higher Cl^- concentrations following the recharge events when all other wells experienced dilutions. Given the lack of a response in Cl^- concentrations, well 6 was interpreted as not receiving input from the upgradient tiles.

Recorded peak concentrations were observed on either day 33 or 37 of the test despite the recharge events on days 24 and 34 that diluted concentrations in the well waters (Figure 2 and Table 1). Velocities for waters traveling from the tiles to the wells, calculated from Eq. (1), ranged from 0.03 to 0.34 m/day with a mean groundwater velocity of 0.19 m/day (Figure 3 and Table 2). Using Eq. (2), the calculated velocity values, a horizontal gradient of 0.002, and an effective porosity of 0.032, a magnitude lower

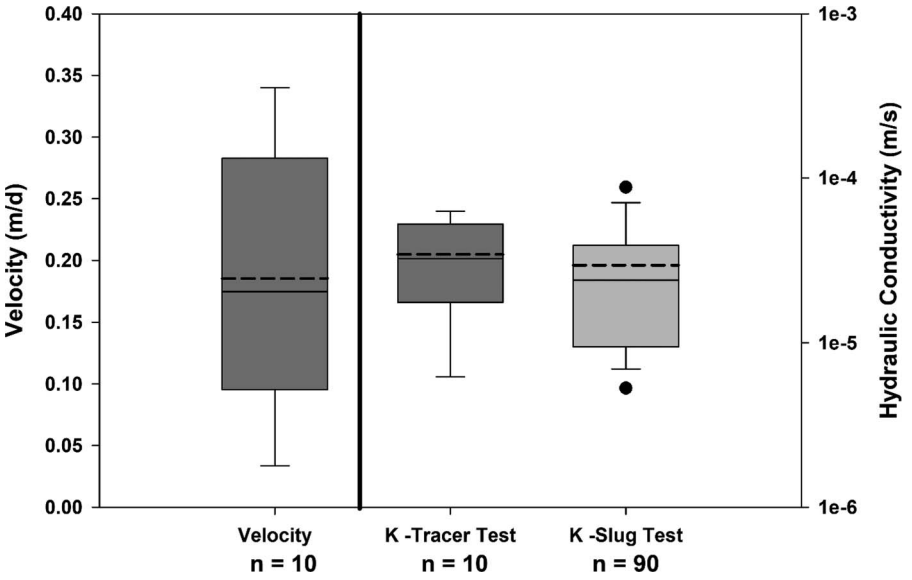

Figure 3. Box and whisker plots for the groundwater velocities calculated using the peak chloride arrival times (t_p) with a comparison of hydraulic conductivity values generated from the tracer test and from slug tests conducted in the wells. The ends of the boxes represent the 25th and 75th percentiles with the solid line at the median and the dashed line at the mean; the error bars depict the 10th and 90th percentiles, and the points represent the 5th and 95th percentiles. Dashed line represents the mean value.

than the measured porosity (Sanks et al., 2015), the hydraulic conductivity (K) values ranged from 5.31×10^{-6} m/s to 6.32×10^{-5} m/s (Figure 3). Among the wells, no significant difference was observed between the K values obtained from the tracer test ($M = 3.43 \times 10^{-5}$, $SD = 1.95 \times 10^{-5}$) and K values calculated from the slug test ($M = 2.65 \times 10^{-5}$, $SD = 2.02 \times 10^{-5}$; $t(5) = 0.741$, $p = 0.492$). The similarity between the tracer hydraulic conductivity and slug test hydraulic conductivity values provided validation of the tracer test results.

End Member Mixing Model

Results from the mixing model are grouped into two sets. The first set resulted from quantifying the proportion of tile water to groundwater in the waters received in the downgradient wells (Eq. 5), and the second set was generated by calculating the expected (modeled) concentration of the NO_3-N in the well water given the mixing of waters (Eq. 6). The difference between the modeled concentration and the measured concentration in the well water indicated either an addition or a removal of NO_3-N. To calculate the proportion of tile water to groundwater, the time to peak concentration (t_p) was incorporated by using concentrations of tile water (Cl_t) and groundwater (Cl_g) t_p days prior to the day of sampling, using the concentration measured in the well (Cl_w) for the day of the sampling. To determine Cl_t for the days in which a sampling was not performed, the concentrations were linearly interpolated between the preceding and following sampled concentrations dates. The time series nature of

Table 2. *Time to peak (t_p), tracer velocities, and hydraulic conductivity values for the downgradient wells.*

				Hydraulic Conductivity (K)	
Well	Distance from Nearest Tile (m)	Time to Peak (t_p) (days)	Tracer Velocity (m/day)	Tracer Test (m/s)	Slug Test (m/s)
8C	3.74	37	0.10	1.87 × 10-5	NA
8D	3.74	37	0.10	1.87 × 10-5	1.32 × 10-5
10C	8.83	33	0.27	4.96 × 10-5	NA
10D	8.50	37	0.23	4.25 × 10-5	4.97 × 10-5
12C	12.63	37	0.34	6.32 × 10-5	1.80 × 10-5
12D	12.13	37	0.33	6.07 × 10-5	6.07 × 10-5
19	2.87	37	0.08	1.44 × 10-5	1.64 × 10-5
20	6.34	37	0.17	3.17 × 10-5	NA
21	4.250	33	0.13	2.38 × 10-5	NA
22	1.06	37	0.03	5.31 × 10-6	7.38 × 10-6

NA = no slug tests have been completed within the well.

Table 3. *Ratios of tile water (Q_t) relative to the groundwater (Q_w) calculated in the sampled wells.*

	$\frac{Qt}{Qw}$		
Well	Minimum	Mean ± Standard Deviation	Maximum
8C	0.19	0.37 ± 0.12	0.57
8D	0.17	0.39 ± 0.10	0.50
10C	0.24	0.32 ± 0.06	0.51
10D	0.23	0.42 ± 0.16	0.71
12C	0.47	0.53 ± 0.08	0.68
12D	0.43	0.49 ± 0.08	0.65
19	0.09	0.24 ± 0.18	0.59
20	0.29	0.40 ± 0.14	0.66
21	0.33	0.45 ± 0.12	0.72
22	0.10	0.22 ± 0.17	0.56

the samples collected generally exhibit temporal continuity, so using that method of interpolation was logical. This methodology resulted in a limited set of the data because the calculation of NO_3-N concentrations could only start after the day the Cl^- arrived at a given well. Thus, results of the mixing model start the day of the observed peak (t_p).

The mixing of tile water and groundwater varied spatially and temporally during the duration of the test. Among the wells, mean ratios (Q_t/Q_w from Eq. [5]) ranged from 0.09 to 0.72 (Table 3). The variability of the ratios suggested heterogeneities within the medium had an influence on the mixing that occurs within the SRB. Modeled NO_3-N_w concentrations for the downgradient wells, Eq. (6), indicated that the SRB both contributed and removed nitrate to and from the system (Figure 4 and Table 4). Up to day 43, wells 8D, 10C, 10D, 12C, 12D, and 20 experienced measured concentrations that were two times larger than the predicted concentrations, indicating that nitrate was added to the system (Figure 4). In the four other wells, measured NO_3-N concentrations were below the modeled concentrations. By day 47, waters in all the wells recorded NO_3-N concentrations below the modeled concentrations, signifying a loss of nitrate in the system.

Dissolved Oxygen

The DO concentrations in the downgradient wells ranged from 0.88 to 11.21 mg/L (Figure 5). Pre-test and early DO concentrations were generally the highest observed concentrations. Concentrations began to decrease following day 7. At day 36, only wells 10C and 19 had DO concentrations higher than 4.5 mg/L, and by day 52, all wells had concentrations less than 4.5 mg/L.

DISCUSSION

During the tracer test, all water entering the control structure was redirected into the diversion tiles. The two-component mixing model verified that the downgradient wells received tile waters that had mixed with the incoming groundwaters. The incorporation of the tile water into the groundwater was not uniform throughout the system as noted by the spatially variable ratio of tile water to groundwater calculated for the wells. The variability could be a result of either heterogeneity of the glacial materials or a function of the error associated with the interpolation of Cl^- concentrations required to ensure the correct lag time. There is the limitation of using a two-component mixing model when the frequency of sampling is not optimal (Anderson et al., 2014), but we feel the observed nitrate losses provided viable results, which aligned with other studies (Utt et al., 2015; Jaynes and Isenhart, 2019).

The mixing model results identified periods of nitrate addition and removal by the SRB. The nitrate removal ranged from 23 to 97 percent. Whereas this is a large range, the values are consistent with other reported values. Utt et al. (2015) reported that nitrate reductions range from 23 ± 28 percent in the SRBs within the Midwest. In the fall fallow season, Brooks and Jaynes (2017) documented a 61 percent reduction. Jaynes and Isenhart (2019) provided the most comprehensive saturated buffer assessment to date with monitoring of six saturated buffers in Iowa. They reported annual nitrate loss ranging from 7 to 92 percent in individual years and averaged 44 ± 26 percent (median, 35 percent) across all site years. In a review paper, Johnson et al. (2023) summarized from five studies with proper designs total N load reductions ranging from 7 to 92 percent.

With all tile water diverted into the system, the SRB had the potential to remove a significant quantity of the nitrate transported within the agricultural discharge. Nitrate removal could occur via denitrification of nitrate to N_2 or N_2O gas, plant uptake, microbial assimilation, and dissimilatory nitrate reduction to ammonium (Lutz et al., 2020). These processes take time to occur, and the time required for tile waters to move through the SRB is an important aspect for the utilization of SRBs as a nutrient-reduction strategy. While quantifying the effectiveness of an SRB to reduce tile NO_3-N concentrations in eastern Iowa, Streeter and Schilling (2021) reported denitrification began to occur within less than a day. Within a span of 7 days, they reported a 10-fold reduction from 15 mg/L NO_3-N to 1.5 mg/L. Applying their results to this work, the observed travel times of 33 to 37 days for waters from the diversion tiles to the wells should have provided sufficient time for removal of nitrate within the T3 SRB.

The transport and behavior of nitrate reflects the conditions within the SRB. As the tile began to flow and saturate the vadose zone, the DO concentrations within the waters reflected aerobic conditions conducive to nitrification. Within the studied SRB, previous works observed increased concentrations of NO_3-N in water during the

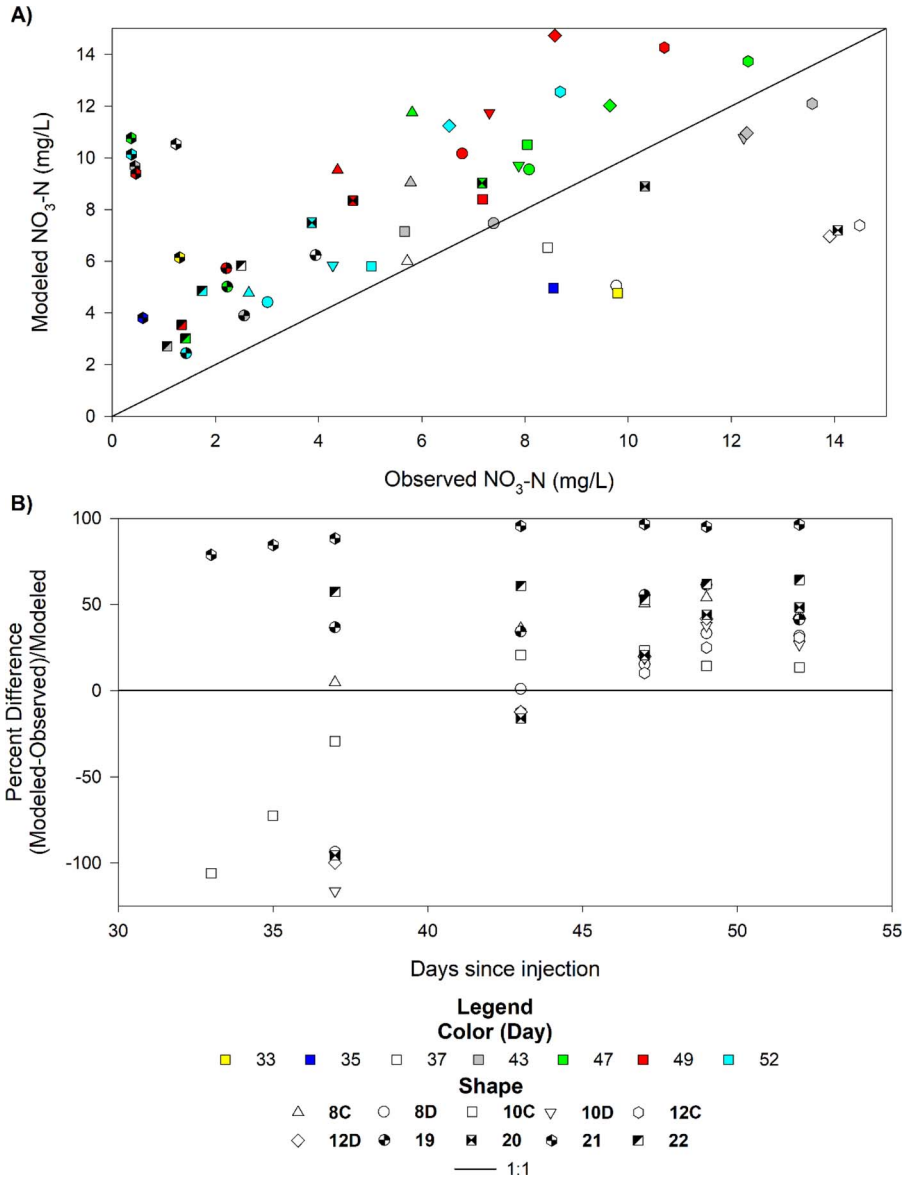

Figure 4. (A) Model nitrate as nitrogen (NO_3-N) concentrations versus observed NO_3-N concentrations in waters of the wells for days 33–52. Points below the 1:1 line indicate addition of nitrate, and points above represent removal of nitrate. (B) Percentage difference between the modeled and observed NO_3-N concentrations for given days following tracer injection. The positive differences indicate removal (denitrification or plant uptake), and negative differences signify addition (nitrification) of NO_3-N.

non-growing season (Miller et al., 2019; Bosompemaa et al., 2021). Bosompemaa et al. (2021) hypothesized that the degradation of the plant material during the non-growing season generated nitrate in the vadose zone. During multiple 24-hour sampling events in the winter and spring, Miller et al. (2019) observed rising NO_3-N concentrations of the groundwater, attributing the increase to nitrification associated with the assimilation of decaying plant material. The timing of the observations by Miller et al. (2019) represented the same time period as the initiation of the tracer test. Whereas the tile diversion system had been running for a couple of days prior to the start of the test, the unsaturated zone of the SRB was beginning to become saturated. We posited that the nitrate accumulated from the decay and degradation of plant material within the unsaturated zone during the fall and winter was being flushed from the unsaturated zone, contributing to the elevated (above modeled) NO_3-N concentrations. The NO_3-N concentrations above the modeled concentrations were measured in wells with DO concentrations above 4.5 mg/L, the threshold observed for denitrification by Anderson et al. (2014). As the soils of the SRB saturated, DO concentrations decreased, falling below 4.5 mg/L in all well water by the

Table 4. *Difference between modeled concentrations of NO_3-N during the various sampling and the corresponding percentage difference in concentration. Positive values, modeled values were greater than the measured concentrations, suggest the removal of nitrate along the pathway from tile to well, whereas negative values are indicative of nitrate addition along the pathway.*

	Modeled – Measured (mg/L)			Percentage Difference		
Well	Minimum	Mean ± Standard Deviation	Maximum	Minimum	Mean ± Standard Deviation	Maximum
8C	0.29	3.35 ± 2.04	5.93	4.8	38 ± 18	54.1
8D	−4.72	0.32 ± 2.73	3.38	−93.6	−2 ± 47	33.2
10C	−5.04	−0.66 ± 2.65	2.45	−105.9	−19 ± 48	23.4
10D	−9.08	−0.55 ± 4.66	4.43	−116.2	−9 ± 56	37.8
12C	−7.11	0.05 ± 4.06	3.86	−96.3	−9 ± 46	30.7
12D	−6.95	0.98 ± 4.71	6.14	−99.9	−2 ± 53	41.8
19	1.00	2.18 ± 0.92	3.51	36.7	46 ± 11	61.3
20	−6.87	0.17 ± 3.98	3.67	−95.6	0 ± 53	48.3
21	3.21	7.95 ± 2.55	10.39	78.8	91 ± 6	96.6
22	1.59	2.37 ± 0.73	3.34	52.8	59 ± 4	64.2

conclusion of the test (Figure 5). The lower DO concentrations coincided with measured NO_3-N concentrations falling below the modeled concentrations, which indicated a loss or removal of nitrate from the system.

Plant uptake and denitrification have been postulated as means to remove nitrate within the T3 SRB (Miller et al., 2019; Bosompemaa et al., 2021). Denitrification leads to the permanent removal of nitrate, whereas the plant uptake is a temporal removal of nitrate. The occurrence of denitrification requires anaerobic conditions and labile organic carbon. When the agricultural runoff enters the SRB, the runoff displaces oxygen in the soil, creating anaerobic conditions. The average measured dissolved oxygen during the period of the tracer test is 4 mg/L. Streeter and Schilling (2021) observed that denitrification is mostly dominant when the dissolved oxygen rate within an SRB ranges from 2 to 4.5 mg/L. With DO concentrations below 4.5 in the T3 SRB, the study site had the required anaerobic conditions required for denitrification to take place.

A soil organic carbon content greater than 0.75 percent is recommended to induce denitrification (USDA-NRCS, 2018; Jaynes and Isenhart 2019). The surficial materials, the top 1.5 m, of the T3 SRB comprise silts and clays, rich with organic matter. Bosompemaa et al. (2021) reported an average organic matter content at the study site to be 6.0 percent at a depth of 60 cm, indicating that there is sufficient organic matter for denitrification to occur within the study site.

Whereas plant uptake has been proposed as a contributing factor to the observed loss of nitrate within the site, the uptake requires the plants to be growing. As a restored prairie, the study site is dominated by switch grass, which can recover 66 percent of applied nitrogen (Bransby et al., 1998). However, at the initiation of the tracer test, the plants were still dormant. In April, the plants were beginning to emerge from dormancy, and growth was observed. Whereas the removal of nitrate aligns with the reemergence of the plants, an observation consistent with other studies (Munoz et al., 1993; Clément et al., 2003; and Li et al., 2016), the observed reduction of nitrate in wells prior to plant growth supported denitrification as the main removal mechanism (Miller et al., 2019; Lutz et al., 2020). Additional support for denitrification comes from Groh et al. (2019); they reported *in situ* denitrification within SRBs via the acetylene inhibition method and found out that denitrification accounted for between 4 and 77 percent of the total nitrate removed within the SRB.

An expectation would be that waters sampled from wells farther away from diversion tiles would have experienced greater nitrate removal given the extended travel distance and time. However, the wells closer to the diversion tiles experienced greater loss of nitrate. Wells 19 and 22 experienced average removal of nitrate representing 91 and 59 percent of the nitrate delivered from the tile waters, whereas wells farther downgradient, wells 10 and 12, witnessed mean differences representing an addition of nitrate. However, by the end of the test, NO_3-N concentrations for the waters in all wells show a loss of nitrate with maximum loss ranging from 23 to 97 percent. Additionally, similar research conducted by Anderson et al. (2014) showed that there was no strong relationship between the amount of nitrate removed and distance away from diversion tiles. They observed some wells closer to diversion tiles that had higher nitrate removal, and their results compare quite well with the results from our test.

CONCLUSIONS

The results from the tracer test highlighted periods of different nitrate behavior, addition and removal, within the SRB. When the SRB was being saturated at the beginning of the tracer test, the introduced tile waters flushed the vadose of nitrate accumulated from the breakdown of plants. Limited denitrification occurred as the presence of aerobic conditions near wells would prevent denitrification. As the SRB continued to receive tile water, aerobic conditions transitioned toward anerobic conditions, which

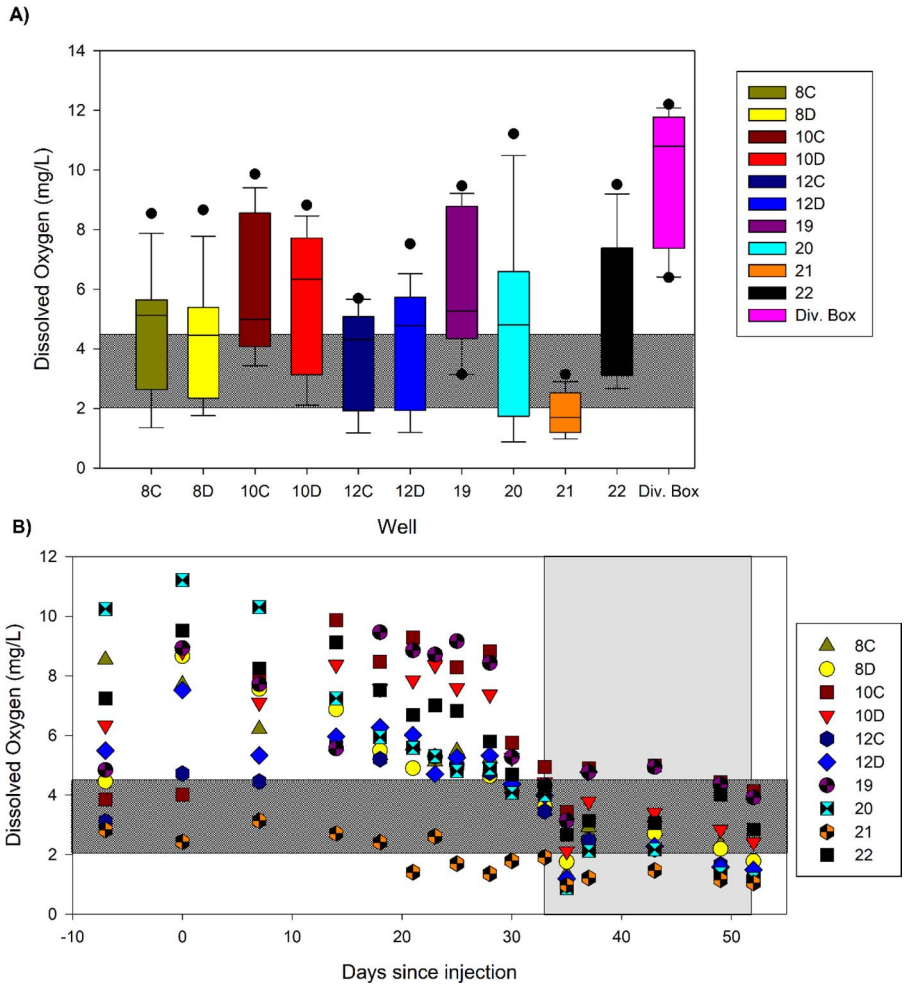

Figure 5. (A) Dissolved oxygen concentrations measured within the well waters for the duration of the tracer tests. (B) Measured dissolved oxygen concentration within the well waters on given sampling dates. Negatives days are pre-test with the injection beginning the tracer test occurring on day 0. The horizontal shaded highlights the concentration from 2 to 4.5 mg/L in both graphs. The vertical shaded area in (B) indicates the period corresponding to the mixing-model results.

corresponded to a coinciding decrease in NO_3-N concentrations that were below the expected NO_3-N concentrations. As time progressed and the plants became more active, greater loss of nitrate was calculated. Overall, the SRB witnessed nitrate reductions between 23 and 97 percent. The observed reductions compared favorably with other published studies exploring SRB and reinforced the effectiveness of SRBs to remove nitrate. Thus, SRBs remain an effective nitrate loss-reduction practice, However, SRBs alone will likely not be sufficient to meet the water quality goals set out by the Illinois Nutrient Loss Reduction Strategy

ACKNOWLEDGMENTS

The authors thank three anonymous reviewers for their comments and feedback, which have improved the paper. This research was funded by the Illinois Water Resources Center, grant number 079901-17840. The authors thank the City of Bloomington (IL) for access to the study location. All authors contributed to the study conception and design. Material preparation and data collection by A.S. and E.W.P. Data analysis and visualizations by A.S. and E.W.P. The first draft of the manuscript was written by A.S. with A.S. and E.W.P. working on the final paper. All authors read and approved the final manuscript.

REFERENCES

Akara, M.; Bruening, B.; Chabela, L. P.; Francis, A. K.; Happel, A.; Hawn, W.; Kisfalusi, Z. D.; Meister, P.; Miller, J.; Rhoads, M.; O'Reilly, C.; Peterson, E. W.; and Twait, R., 2016, Groundwater flow along a gravel-sand lense in a glaciated terrain. *Geological Society of America Annual Meeting*, Denver, CO, 2016, Vol. 48: Geological Society of America, doi:10.1130/abs/2016AM-285159

Anderson, T. R.; Groffman, P. M.; Kaushal, S. S.; and Walter, M. T., 2014, Shallow groundwater denitrification in riparian zones of a headwater agricultural landscape: *Journal Environmental Quality*, Vol. 43, pp. 732–744.

Becker, J. P. and Peterson, E. W., 2022, Stream recovery post channelization: A case study of low-gradient streams in central Illinois, USA: *Hydrology*, Vol. 9, p. 160.

Bosompemaa, P.; Peterson, E. W.; Perry, W.; and Seyoum, W. M., 2021, Recycling of nitrate and organic matter by plants in the vadose zone of a saturated riparian buffer: *Water Air and Soil Pollution*, Vol. 232, No. 245, pp. 14, doi:10.1007/s11270-021-05202-3

Bransby, D.; McLaughlin, S.; and Parrish, D., 1998, A review of carbon and nitrogen balances in switchgrass grown for energy: *Biomass Bioenergy*, Vol. 14, pp. 379–384.

Brooks, F. and Jaynes, D., 2017, *Quantifying the effectiveness of installing saturated buffers on conservation reserve program to reduce nutrient loading from tile drainage waters*: United States Department of Agriculture, AG-3151-P-16-0225, 55 p.

Carstensen, M. V.; Hashemi, F.; Hoffmann, C. C.; Zak, D.; Audet, J.; and Kronvang, B., 2020, Efficiency of mitigation measures targeting nutrient losses from agricultural drainage systems: A review: *Ambio*, Vol. 49, pp. 1820–1837.

Chandrasoma, J. M.; Christianson, R. D.; and Christianson, L. E., 2019, Saturated buffers: What is their potential impact across the US Midwest? *Agricultural Environmental Letters*, Vol. 4, p. 180059.

Clément, J. C.; Holmes, R. M.; Peterson, B. J.; and Pinay, G., 2003, Isotopic investigation of denitrification in a riparian ecosystem in western France: *Journal Applied Ecology*, Vol. 40, pp. 1035–1048.

David, M. B. and Gentry, L. E., 2000, Anthropogenic inputs of nitrogen and phosphorus and riverine export for Illinois, USA: *Journal Environmental Quality*, Vol. 29, pp. 494–508.

Fausey, N. R.; Brown, L. C.; Belcher, H. W.; and Kanwar, R. S., 1995, Drainage and water quality in Great Lakes and cornbelt states: *Journal Irrigation Drainage Engineering*, Vol. 121, pp. 283–288.

Gentry, L. E.; David, M. B.; Smith, K. M.; and Kovacic, D. A., 1998, Nitrogen cycling and tile drainage nitrate loss in a corn/soybean watershed: *Agriculture Ecosystems Environment*, Vol. 68, pp. 85–97.

Groh, T. A.; Davis, M. P.; Isenhart, T. M.; Jaynes, D. B.; and Parkin, T. B., 2019, In situ denitrification in saturated riparian buffers: *Journal Environmental Quality*, Vol. 48, pp. 376–384.

Hautman, D. P. and Munch, D. J. J. E. O., 1997, Method 300.1: *Determination of inorganic anions in drinking water by ion chromatography*: U.S. Environmental Protection Agency, Cincinnati, OH, 40 p.

Hypoxia Task Force, 2018, *Progress report on coordination for nonpoint source measures in hypoxia task force states*: U.S. Environmental Protection Agency, 39 p.

Illinois Environmental Protection Agency; Illinois Department of Agriculture; and University of Illinois Extension, 2019, *Illinois Nutrient Loss Reduction Strategy biennial report 2017-2018*, IISG19-RCE-RLA-071, Springfield, IL.

Jaynes, D. B. and Isenhart, T. M., 2014, Reconnecting tile drainage to riparian buffer hydrology for enhanced nitrate removal: *Journal Environmental Quality*, Vol. 43, pp. 631–638.

Jaynes, D. B. and Isenhart, T. M., 2019, Performance of saturated riparian buffers in Iowa, USA: *Journal Environmental Quality*, Vol. 48, pp. 289–296.

Johnson, G.; Christianson, L.; Christianson, R.; Davis, M.; Díaz-García, C.; Groh, T.; Isenhart, T.; Kjaersgaard, J.; Malone, R.; Pease, L. A.; and Rogovska, N., 2023, Effectiveness of saturated buffers on water pollutant reduction from agricultural drainage: *Journal Natural Resources Agricultural Ecosystems*, Vol. 1, pp. 49–62.

Kaur, G.; Zurweller, B. A.; Nelson, K. A.; Motavalli, P. P.; and Dudenhoeffer, C. J., 2017, Soil waterlogging and nitrogen fertilizer management effects on corn and soybean yields: *Agronomy Journal*, Vol. 109, pp. 97–106.

Keeney, D. R. and Hatfield, J. L., 2008, The nitrogen cycle, historical perspective, and current and potential future concerns. In Hatfield, J. L. and Follett, R. F. (Editors), *Nitrogen in the Environment* (Second Edition), Academic Press, San Diego, pp. 1–18.

Lemke, A. M.; Kirkham, K. G.; Lindenbaum, T. T.; Herbert, M. E.; Tear, T. H.; Perry, W. L.; and Herkert, J. R., 2011, Evaluating agricultural best management practices in tile-drained subwatersheds of the Mackinaw River, Illinois: *Journal Environmental Quality*, Vol. 40, pp. 1215–1228.

Li, X.; Rennenberg, H.; and Simon, J., 2016, Seasonal variation in N uptake strategies in the understorey of a beech-dominated N-limited forest ecosystem depends on N source and species: *Tree Physiology*, Vol. 36, pp. 589–600.

Lutz, S. R.; Trauth, N.; Musolff, A.; Van Breukelen, B. M.; Knöller, K.; and Fleckenstein, J. H., 2020, How important is denitrification in riparian zones? Combining end-member mixing and isotope modeling to quantify nitrate removal from riparian groundwater: *Water Resources Research*, Vol. 56, p. e2019WR025528.

Mattingly, R. L.; Herricks, E. E.; and Johnston, D. M., 1993, Channelization and levee construction in Illinois: Review and implications for management: *Environmental Management*, Vol. 17, pp. 781–795.

Miller, J.; Peterson, E. W.; and Budikova, D., 2019, Diurnal and seasonal variation in nitrate-nitrogen concentrations of groundwater in a saturated buffer zone: *Hydrogeology Journal*, Vol. 27, pp. 1373–1387.

Miller, J. D.; Schoonover, J. E.; Williard, K. W. J.; and Hwang, C. R., 2011, Whole catchment land cover effects on water quality in the lower Kaskaskia River Watershed: *Water Air Soil Pollution*, Vol. 221, pp. 337–350.

Munoz, N.; Guerri, J.; Legaz, F.; and Primo-Millo, E., 1993, Seasonal uptake of 15 N-nitrate and distribution of absorbed nitrogen in peach trees: *Plant soil*, Vol. 150, pp. 263–269.

Peterson, B. J.; Wollheim, W. M.; Mulholland, P. J.; Webster, J. R.; Meyer, J. L.; Tank, J. L.; Martí, E.; Bowden, W. B.; Valett, H. M.; Hershey, A. E.; McDowell, W. H.; Dodds, W. K.; Hamilton, S. K.; Gregory, S.; and Morrall, D. D., 2001, Control of nitrogen export from watersheds by headwater streams: *Science*, Vol. 292, pp. 86–90.

Robertson, D. M. and Saad, D. A., 2013, SPARROW models used to understand nutrient sources in the Mississippi/Atchafalaya River Basin: *Journal Environmental Quality*, Vol. 42, pp. 1422–1440.

Sanks, K.; Peterson, E. W.; Taye, T.; O'Reilly, C.; Kisfalusi, Z. D.; Rothschild, T. J.; and Twait, R., 2015, Understanding the amount of nitrate in relation to percent of organic matter in riparian buffer zone soils at stream T3 in Hudson, Illinois: *Abstracts with Programs*, Geological Society of America, Baltimore, MD, Vol. 47, No. 7, p. 534.

Streeter, M. T. and Schilling, K. E., 2021, Quantifying the effectiveness of a saturated buffer to reduce tile NO_3-N concentrations in eastern *Iowa:* Environmental Monitoring Assessment, Vol. 193, p. 500.

Triska, F. J.; Kennedy, V. C.; Avanzino, R. J.; Zellweger, G. W.; and Bencala, K. E., 1989, Retention and transport of nutrients in a third-order stream in northwestern California: Hyporheic processes: *Ecology*, Vol. 70, pp. 1893–1905.

U.S. Department of Agriculture–Natural Resources Conservation Service, 2018, *Conservation practice standard, saturated buffer, code 604. USDA-NRCS field office technical guide*: Bismarck, ND, 4 p.

U.S. Environmental Protection Agency, 2017, *Mississippi River/Gulf of Mexico Watershed Nutrient Task Force 2017 Report to Congress*: Washington, DC, 121 p.

Utt, N.; Jaynes, D.; and Albertsen, J., 2015, Demonstrate and evaluate saturated buffers at field scale to reduce nitrates and phosphorus from subsurface field drainage systems: *Mississippi River Basin Water Management*, pp. 1–74.

Weedman, N. R.; Malone, D. H.; and Shields, W. E., 2014, *Surficial geologic map of the Normal West 7.5 Minute Quadrangle, McLean County, Illinois, 2014 GSA Annual Meeting*: Vancouver, British Columbia.

Wickham, S. S.; Johnson, W. H.; and Glass, H. D., 1988, *Regional geology of the Tiskilwa till member, Wedron formation*, northeastern Illinois: Circular no. 543.